

Supporting Information

Effect of Cosolvents on the Phase Separation of Polyelectrolyte Complexes

Yuanchi Ma^{a,*}, *Robert J. S. Ivancic*^b, *Jan Obrzut*^b, *Debra J. Audus*^b, *Vivek M. Prabhu*^{b,*}

^a. College of Polymer Science and Engineering, Qingdao University of Science and Technology, Qingdao, Shandong, China

^b. Materials Science and Engineering Division, Material Measurement Laboratory, National Institute of Standards and Technology, 100 Bureau Drive, Gaithersburg, MD, United States

Section I. Dielectric Constant Measurement

Details of the dielectric measurements were described in the main text. The cosolvents, ethylene glycol (EG) and N-methylformamide (NMF), were selected, since they are both miscible with water and have moderate solubilities to the two polyelectrolytes and the salt (KBr). To summarize, the real (ϵ') and imaginary (ϵ'') parts of the dielectric constant were plotted on the Cole-Cole complex plane, and in all cases, the data show typical shape of Cole-Cole semi-circles (**Figure 5a**, showed the binary mixture NMF/H₂O, as an example). In order to determine ϵ_0 , we employed the single dielectric relaxation model of Debye:

$$\epsilon''(\omega) = \frac{(\epsilon_0 - \epsilon_\infty)\omega\tau}{1 + \omega^2\tau^2} \quad (\text{S1})$$

which can be rearranged to give:

$$\omega\epsilon''(\omega) = \frac{1}{\tau}(\epsilon_0 - \epsilon'(\omega)) \quad (\text{S2})$$

Figure S1 demonstrate the linear relationship of $\omega\epsilon''$ and ϵ' denoted by equation S2 for the solvent mixtures of EG/H₂O. Consequently, the static dielectric constants ϵ_0 can be determined from the horizontal intercepts.

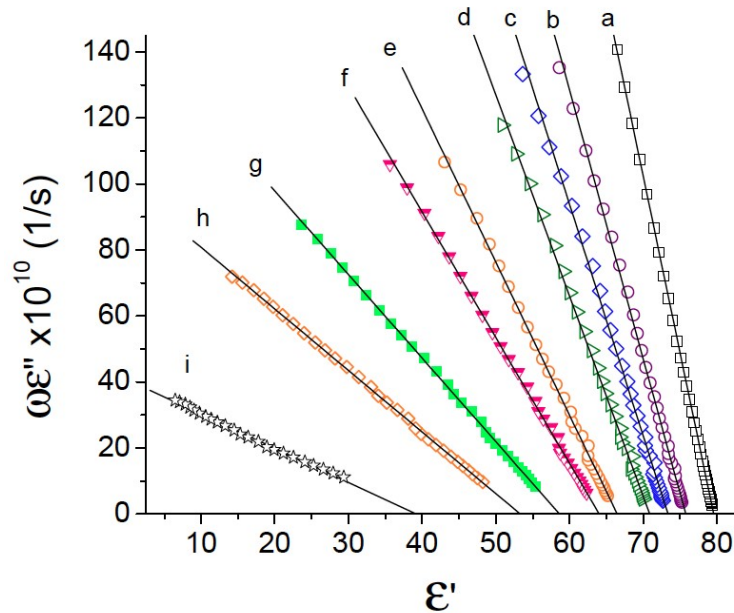


Figure S1. Plots of equation S2, $\omega\epsilon''(\omega)$ vs $\epsilon'(\omega)$, for the following volume concentrations of EG in H₂O: (a) 0 (pure water), (b) 13.1 %, (c) 20.8 %, (d) 28.3 %, (e) 40.8 %, (f) 48.5 %, (g) 63.2 %, (h) 75.0 %, (i) 100% (pure EG). Solid lines are linear fits through the data points.

Uncertainty evaluation

Uncertainty was estimated by the quadrature method, which yields a standard uncertainty estimate (with a 68 % confidence interval) and is especially useful and effective in the case of several variables that weight the uncertainty non-uniformly. Here, the relative uncertainties in the broadband dielectric measurements are within 2 % of the measured ε'' and ε' values. The standard errors estimated from the least-square linear fitting of ε_0 results, $\Delta\varepsilon_{0,\text{fit}}$, are within ± 0.25 (Figure 5b, 5c and Figure S1). The combined standard uncertainty, estimated from the square root of quadrature model,¹ is obtained from equation S3:

$$\Delta\varepsilon_0/\varepsilon_0 = [((\Delta\varepsilon'')/\varepsilon'')^2 + ((\Delta\varepsilon')/\varepsilon')^2 + ((\Delta\varepsilon_{0,\text{fit}})/\varepsilon_0)^2]^{1/2} \quad (\text{S3})$$

The measured ε_0 values and their calculated errors (Err \pm) obtained for the two binary and the one ternary mixtures are summarized in Table S1 – S3, and illustrated in Figure S2.

Table S1. Static dielectric constant, ε_0 , of the NMF/H₂O mixtures

Vol fraction % of NMF in H ₂ O	ε_0	Err \pm
0	79.6	1.8
16.7	84.0	1.9
25.7	86.5	2.0
36.9	90.1	2.1
48.7	95.1	2.2
59.2	101.1	2.3
67.2	107.6	2.5
78.7	120.0	2.8
85.0	131.6	3.1
100	176.2	4.2

Table S2. Static dielectric constant, ε_0 , of the EG/H₂O mixtures

Vol fraction % of EG in H ₂ O	ε_0	Err \pm
0	79.6	1.6
13.1	75.8	1.7
20.8	73.4	1.7
28.8	70.9	1.6
40.8	66.8	1.5
48.5	64.0	1.4
63.2	58.7	1.2
85.0	53.3	1.1
100	39.2	1.0

Table S3. Static dielectric constant, ϵ_0 , of the EG/NMF/H₂O mixtures

Vol fraction % of EG: NMF: H ₂ O	ϵ_0	Err \pm
33.4 : 52.4 : 14.2	69.3	1.5
17.0 : 76.2 : 6.8	75.6	1.7

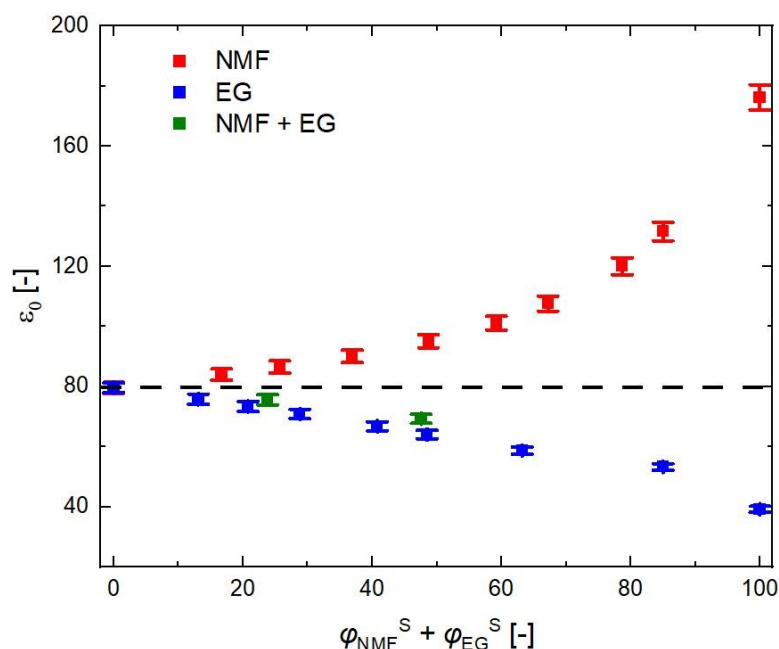
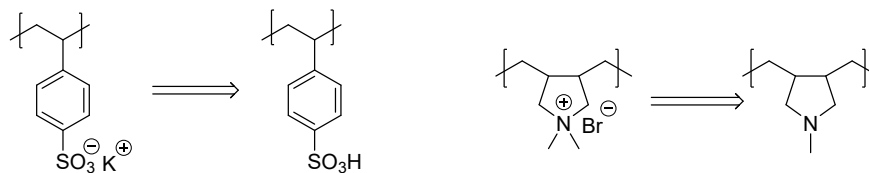


Figure S2. Summary of the dielectric constants (ϵ_0) of the binary and ternary solvent mixtures as a function of $(\varphi_{EG}^S + \varphi_{NMF}^S)$ as measured by dielectric experiments (φ^S denotes the cosolvent volume fraction relative to the total solvent volume). The dashed line marks the dielectric constant of pure water, for visual aid only.

Section II. Estimation of χ by Group Contribution Method

Potassium poly(styrene sulfonate) (KPSS) and poly(diallyldimethylammonium) bromide (PDADMAB) structures were approximated by group contribution methods in the form of their uncharged equivalent structures, PSS⁻ and PDADMA⁺, respectively, as shown in Scheme S1.



Scheme S1. The uncharged equivalent structures of PSS⁻ and PDADMA⁺ used in the calculation of solubility parameters.

Table S4. δ_d , δ_p and δ_h of water, EG and NMF.

Solvent	v_m [cm ³ /mol]	δ_d [J ^{1/2} /cm ^{3/2}]	δ_p [J ^{1/2} /cm ^{3/2}]	δ_h [J ^{1/2} /cm ^{3/2}]
H ₂ O	18.1	12.3	31.3	34.2
EG	55.9	17.0	11.0	26.0
NMF	59.1	17.4	18.8	15.9

The Hansen solubility parameter of each molecule is composed of three parts, δ_d , δ_p and δ_h , which represent the dispersion, dipolar, and hydrogen bonding contribution to its cohesive energy density, and act as the coordinates for a point in the 3D space known as the Hansen space. The miscibility of a polymer and a solvent can thus be empirically estimated by the relative distance between the two points in the Hansen space. The δ components of common solvents under room temperature are well-documented in the literature (Table S4),² while those of polymers can be calculated using the following equations (eqs. S4 – S6):

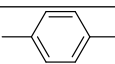
$$\delta_d = \sum F_{d,i}/v_m \quad (\text{S4})$$

$$\delta_p = \sqrt{\sum F_{p,i}^2/v_m} \quad (\text{S5})$$

$$\delta_h = \sqrt{\sum E_{h,i}/v_m} \quad (\text{S6})$$

in which $F_{d,i}$, $F_{p,i}$ and $E_{h,i}$ are the cohesive energy contributions of dispersion force, dipolar interaction and hydrogen bonding from *each group* in a monomer, with the molar volume of v_m .² Table S5 and S6 summarize the group contributions of $F_{d,i}$, $F_{p,i}$ and $E_{h,i}$ in PSS and PDADMA, respectively.

Table S5. Group contributions of $F_{d,i}$, $F_{p,i}$ and $E_{h,i}$ in PSS.²

Group	Number	$F_{d,i}$ [J ^{1/2} cm ^{3/2} mol ⁻¹]	$F_{p,i}^2$ [J cm ³ mol ⁻²]	$E_{h,i}$ [J mol ⁻¹]
-CH ₂ -	1	270	0	0
-CH<	1	80	0	0
	1	1270	12100	0
-SO ₂ - ³	1	597	2117025	11347
-OH	1	210	250000	20000
Total		2427	2379125	31347

For PSS, $v_m = M_0/\rho = 184/1.11 = 166$ cm³/mol.

Therefore, $\delta_d = 2427/166 = 14.6$ J^{1/2}cm^{-3/2}; $\delta_p = (2379125)^{1/2}/166 = 9.29$ J^{1/2}cm^{-3/2}; $\delta_h = (31347/166)^{1/2} = 13.7$ J^{1/2}cm^{-3/2}.

Table S6. Group contributions of $F_{d,i}$, $F_{p,i}$ and $E_{h,i}$ in PDADMA.²

Group	Number	$F_{d,i}$ [$\text{J}^{1/2}\text{cm}^{3/2}\text{mol}^{-1}$]	$F_{p,i}^2$ [$\text{J cm}^3\text{mol}^{-2}$]	$E_{h,i}$ [J mol^{-1}]
-CH ₂ -	4	270	0	0
-CH<	2	80	0	0
-CH ₃	1	420	0	0
-N<	1	20	640000	5000
Total		1680	640000	5000

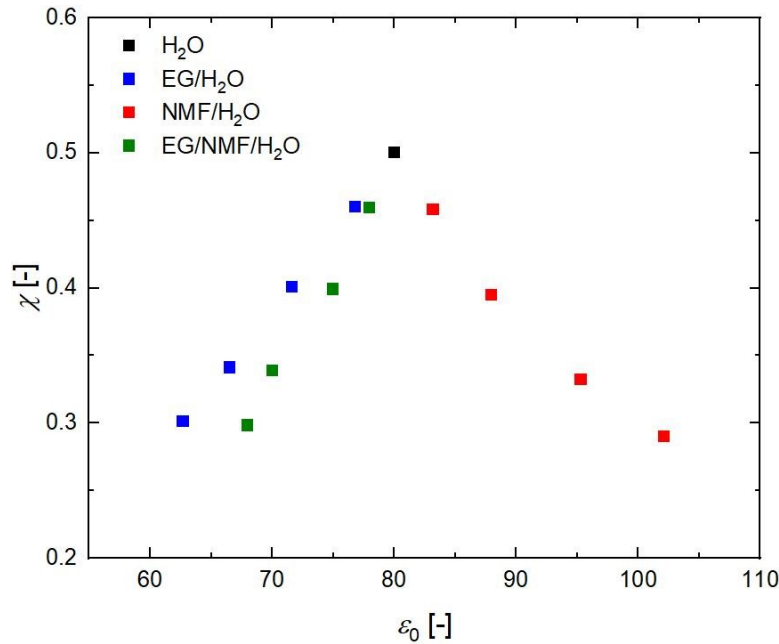
For PDADMA, $v_m = M_0/\rho = 111/1.09 = 102 \text{ cm}^3/\text{mol}$.

Therefore, $\delta_d = 1680/102 = 16.47 \text{ J}^{1/2}\text{cm}^{-3/2}$; $\delta_p = (640000)^{1/2}/102 = 7.84 \text{ J}^{1/2}\text{cm}^{-3/2}$; $\delta_h = (5000/102)^{1/2} = 7.00 \text{ J}^{1/2}\text{cm}^{-3/2}$.

Subsequently, the χ values between the polymers (PSS, PDADMA) and the solvents (H₂O, EG, NMF) can be calculated using equation S7:^{4,5}

$$\chi = \frac{\alpha' l^3}{RT} [(\delta_{d,1} - \delta_{d,2})^2 + 0.25(\delta_{p,1} - \delta_{p,2})^2 + 0.25(\delta_{h,1} - \delta_{h,2})^2] \quad (\text{S7})$$

where α' is a prefactor in the range of zero to unity, R is the ideal gas constant, and T is the temperature in Kelvin. The subscripts 1 and 2 denote the solvent and the polymer, respectively. Here, we explicitly take the reference volume to be $l^3 = 0.0366 \text{ nm}^3$ rather than the typical solvent volume $v_{m,1}$ so that our reference volume is constant throughout the text. By taking $\alpha' = 0.193$ and $T = 293 \text{ K}$, the results of χ are summarized in Table 2 of the main text, and their relations to the dielectric constants are shown in Figure S3.

**Figure S3.** χ as a function of ϵ_0 for the solvent mixtures.

Section III. Voorn-Overbeek (VO) Modelling of the Experimental Data

Parameterization of VO model at 293 K

VO theory is used to describe the phase separation of KPSS-PDADMAB complexes:

$$\frac{l^3 f(\varphi_p, \varphi_s)}{V k T} = \frac{\varphi_p}{N} \ln \left(\frac{\varphi_p}{2} \right) + \varphi_s \ln \left(\frac{\varphi_s}{2} \right) + \varphi_0 \ln \varphi_0 + \chi \varphi_p \varphi_0 - \alpha (\varphi_s + \sigma \varphi_p)^{3/2} \quad (\text{S8})$$

As an on-lattice theory, VO in their original publications⁶ defined the parameter N as the number of lattices that a polymer chain occupies, and therefore $N = DP \cdot (v_m/l^3)$ where DP , v_m and l^3 are the degree of polymerization, monomer volume and reference volume. The reference volume is taken to be the lattice size cubed ($l^3 = 0.0366 \text{ nm}^3$). Similarly, the polymer charge density σ is also corrected by this volume ratio, which follows $\sigma = z/N = (z/DP)/(v_m/l^3)$, where z is the net charges per polymer chain. In this study, we take the harmonic mean of the DP of KPSS and PDADMAB,⁷ which gives the average degree of polymerization (DP^*) of $[2/(1/315+1/107)] = 160$. As both KPSS and PDADMAB are strong polyelectrolytes, with charge densities (z/DP) close to 1; $v_m/l^3 = 6.4$. Therefore, we used $N = 160 \times 6.4 = 1025 \approx 1000$, and $\sigma = 1/6.4 = 0.156 \approx 0.1$ in the calculation, as stated in the main text.

The ε_0 and χ used to construct Figure 2a in the main text are summarized in Table S7; VO predicts positive tie lines for all binodal curves, and a few representatives are shown in Figure S4 (these details are omitted in Figure 2a for clarity).

Table S7. Parameters used in VO model at 293 K.

Solvent composition	$\varphi_{\text{EG}}^{\text{S}}$ or $\varphi_{\text{NMF}}^{\text{S}}$ [-]	ε_0 [-]	χ [-]
EG + H ₂ O	0.50	62.7	0.302
	0.40	66.5	0.341
	0.25	71.6	0.401
	0.10	76.8	0.460
H ₂ O	0	80.0	0.500
NMF + H ₂ O	0.10	83.2	0.458
	0.25	88.0	0.395
	0.40	95.3	0.332
	0.50	102.1	0.290

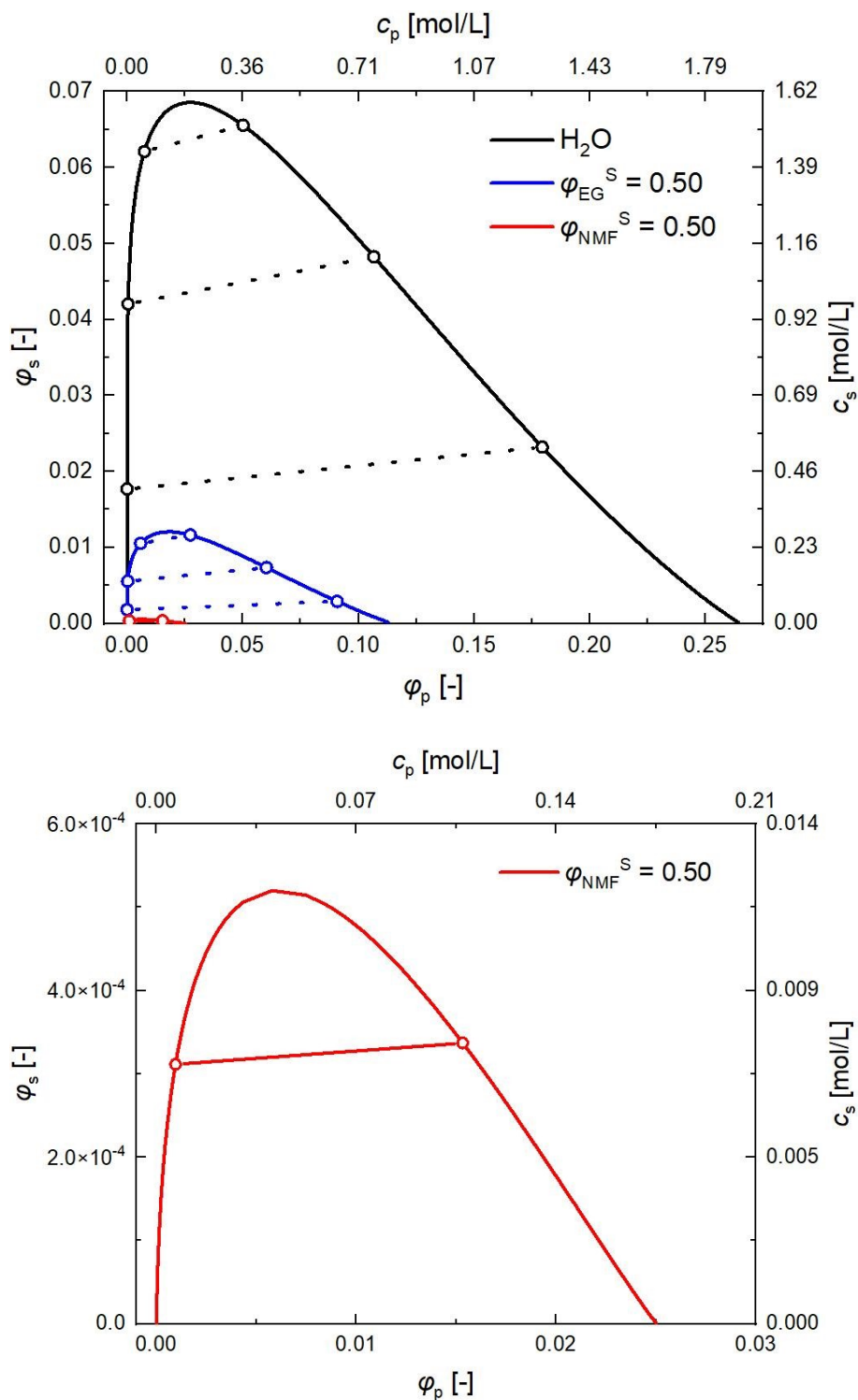


Figure S4. Top: representative VO phase diagrams (solid lines) of KPSS-PDADMAB complexes in pure H₂O (black), EG/H₂O=50/50 (blue), and NMF/H₂O=50/50 (red), showing the tie lines (dashed lines) in each case. Bottom: zoom-in view of the red curve. $T = 293$ K.

Parameterization of VO model at 313 and 333 K

$\epsilon_0(T)$ of pure water,¹⁰ EG¹¹ and NMF^{8,9} are available in literature (Figure S5a), and their corresponding Bjerrum lengths, $l_B(T) \sim 1/[\epsilon_0(T) \cdot T]$, all monotonically increase with T (Figure S5b). At elevated temperatures, $\epsilon_0(T)$ of the solvent mixtures can be determined by interpolation of the literature data in Figure S5a. The results are shown in Figure S6 and S7. In Figure S6, the interpolated $\epsilon_{0,\text{EG-H}_2\text{O}}(T)$ at $\varphi_{\text{EG}}^S = 0$ to 0.5 agree well with the values given by Akerlof,¹¹ with difference smaller than 1. In Figure S7, to the best of our knowledge, there are no literature data of $\epsilon_{0,\text{NMF-H}_2\text{O}}(T)$ available above 30 °C. Nevertheless, the interpolated data at $T = 40$ °C and 60 °C are generally in accord with those measured by Rohdewald *et al.*¹² and Sengwa *et al.*¹³

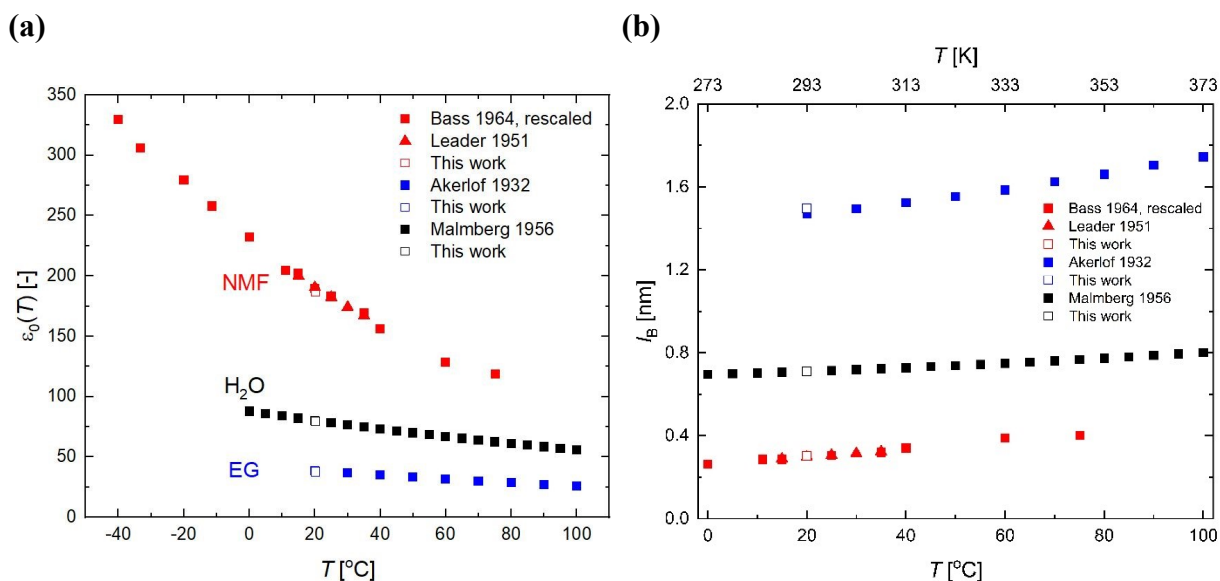


Figure S5. (a) ϵ_0 and (b) l_B as a function of temperature for pure H₂O, EG and NMF. The solid symbols represent the data from literature,^{8,9,10,11} and the open symbols represent the values measured by us. The $\epsilon_{0,\text{NMF}}$ values measured by Bass *et al.*⁸ are multiplied by a factor of 1.07 to be consistent with others.

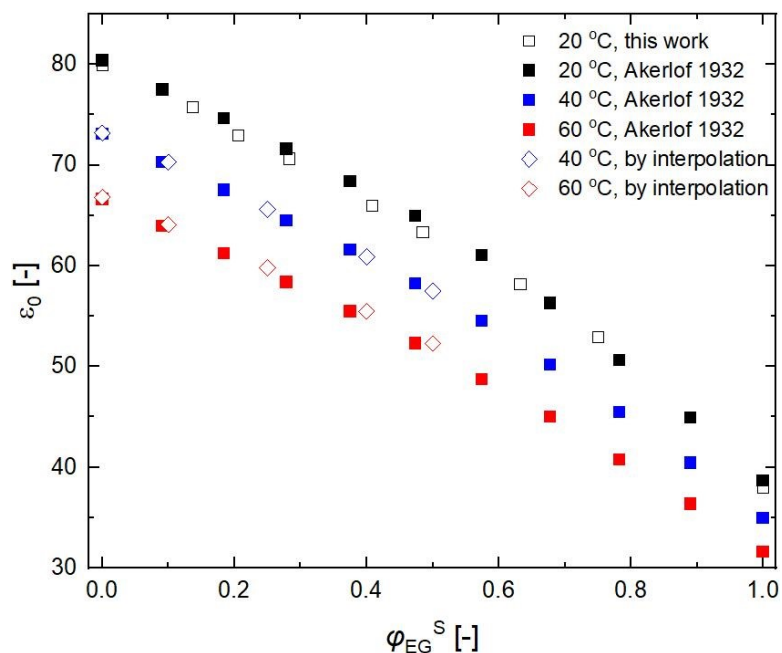


Figure S6. ε_0 as a function of φ_{EG}^S at various T . The solid symbols represent the data from literature.¹¹ The open symbols represent the values calculated by interpolation of Figure S5a datasets with respect to volume fraction.

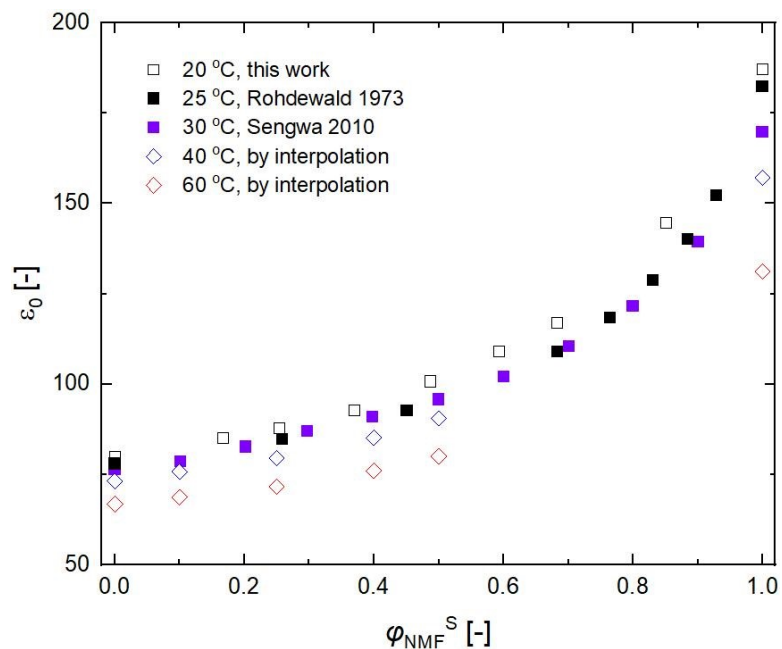


Figure S7. ε_0 as a function of φ_{NMF}^S at various T . The solid symbols represent the data from literature.^{12,13} The open symbols represent the values calculated by interpolation of Figure S5a datasets with respect to volume fraction.

Table S8 summarizes the ε_0 and χ values used to simulate the binodal phase boundaries of polyelectrolyte complexes (PEC) in binary solvent mixtures at 313 K and 333 K. The temperature-dependent solvent dielectric constants [$\varepsilon_0(T)$] were extracted from Figure S6 and S7 (the blue and red diamonds for 313 K and 333 K, respectively). Notably, we parameterized the temperature-dependent $\chi(T)$ as: $\chi(T) = \chi(293)(0.2 \times 293/T + 0.8)$, where $\chi(293) = 0.50, 0.10$ and 0.080 for H₂O, EG and NMF as stated in Table 2 of the main text. The solvent density only weakly depends on T , and therefore was treated as T -independent.

Table S8. Parameters used in VO model at 313 K and 333 K.

Solvent composition	$\varphi_{\text{EG}}^{\text{S}}$ or $\varphi_{\text{NMF}}^{\text{S}}$ [-]	$T = 313 \text{ K}$		$T = 333 \text{ K}$	
		ε_0 [-]	χ [-]	ε_0 [-]	χ [-]
EG + H ₂ O	0.50	57.4	0.298	52.3	0.294
H ₂ O	0	73.2	0.494	66.8	0.488
NMF + H ₂ O	0.50	90.5	0.286	80.1	0.283

The model prediction results are shown in Figure S8. For PEC in H₂O, and 50:50 volume fraction mixtures with EG and NMF, the theoretical phase diagrams shift upward as T increases from 293 K to 333 K, which indicates decreased miscibility and recovers the experimental observation of lower critical solution temperature behaviors. Nonetheless, a stronger $\chi(T)$ function, for example, $\chi(T) = \chi(293)(293/T)$, will make the VO model to predict upper critical solution temperature behaviors, as illustrated in Figure S9.

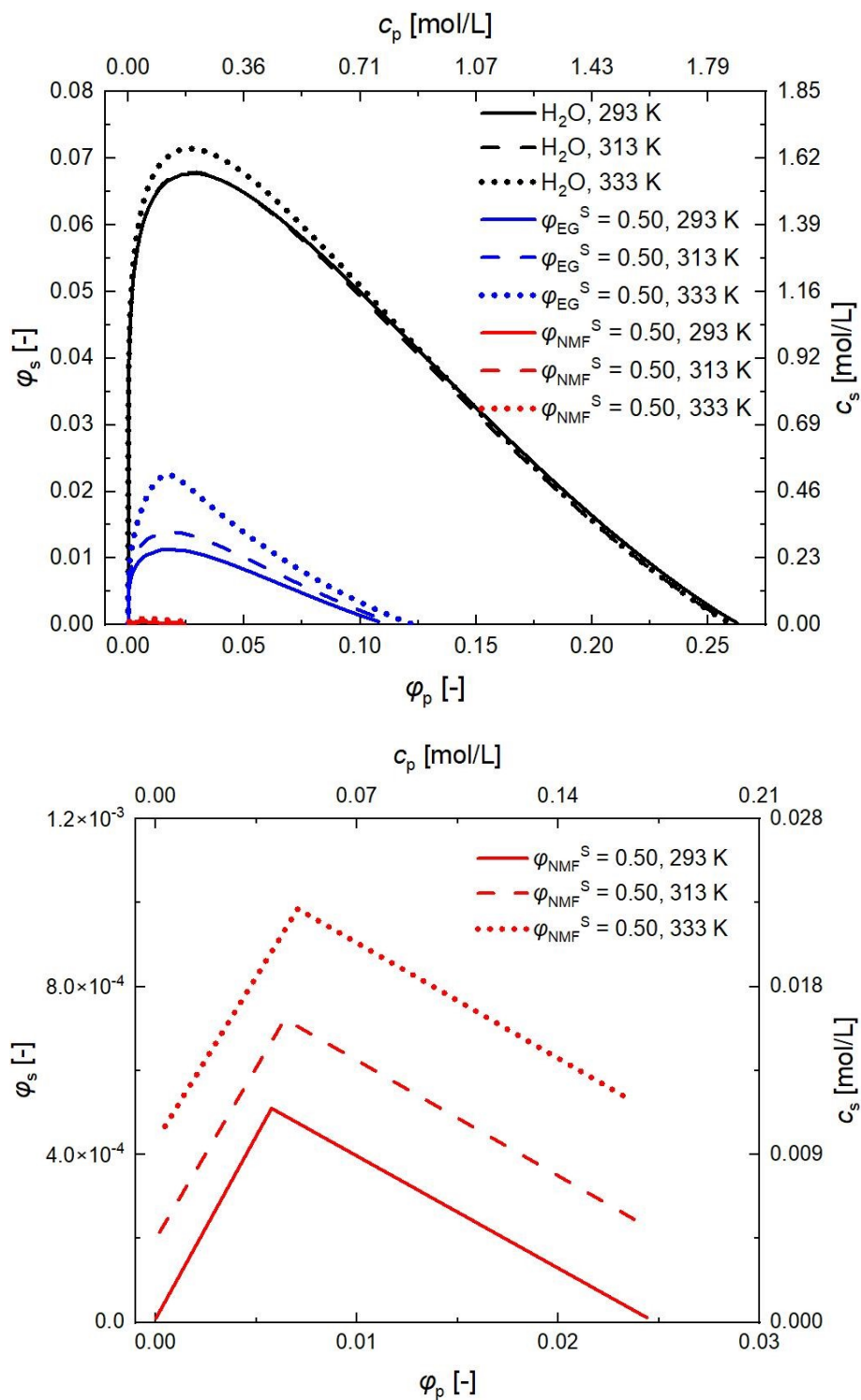


Figure S8. Top: representative theoretical ϕ_s - ϕ_p phase diagrams of three solvent compositions (water, EG/H₂O=50/50, and NMF/H₂O=50/50) at 293 K, 313 K and 333 K, assuming $\chi_{\text{solvent-p}}(T) = \chi_{\text{solvent-p}}(293)(0.2 \times 293/T + 0.8)$. Bottom: zoom-in view of the red curves.

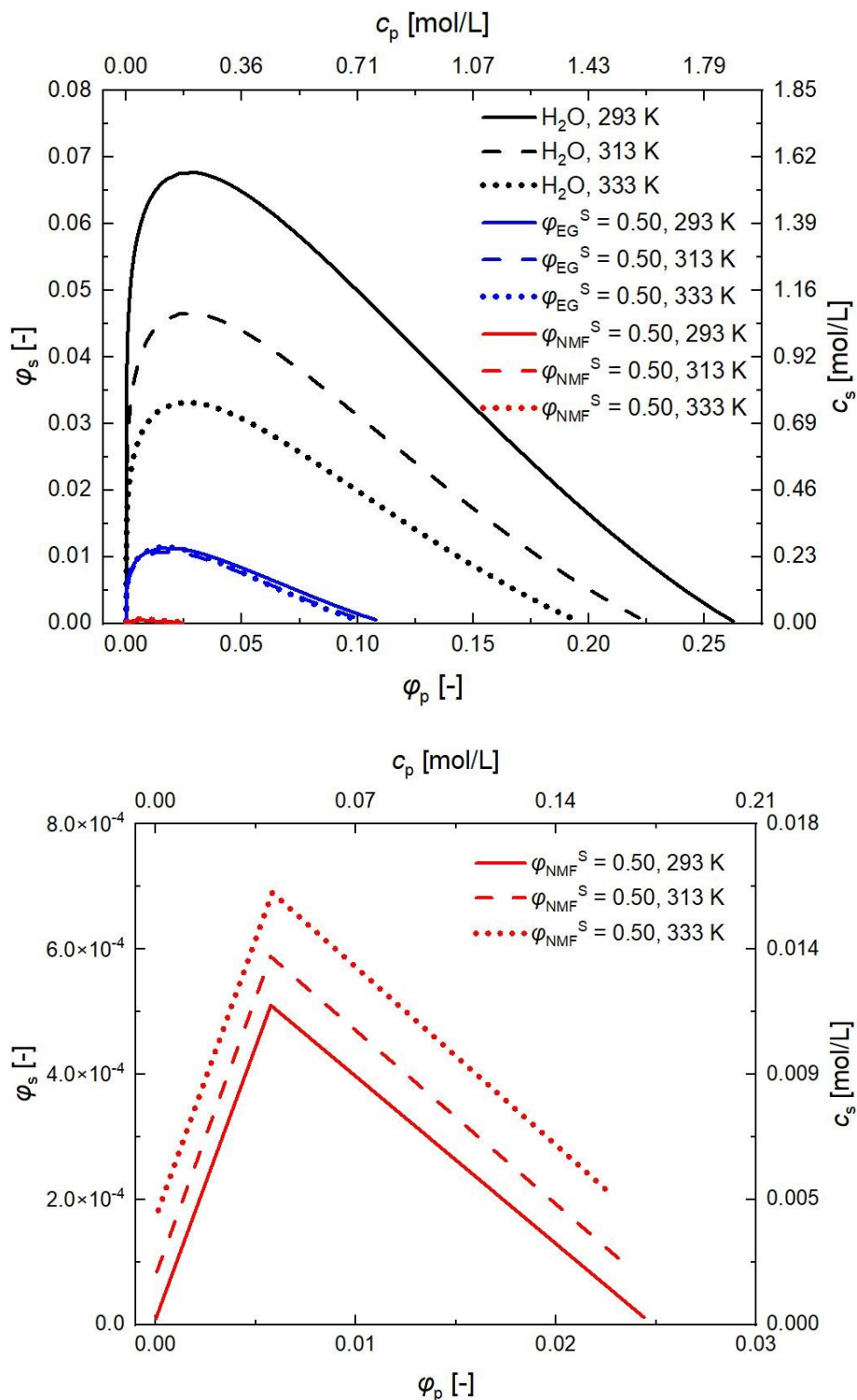


Figure S9. Top: representative theoretical ϕ_s - ϕ_p phase diagrams of three solvent compositions (water, EG/ H_2O =50/50, and NMF/ H_2O =50/50) at 293 K, 313 K and 333 K, assuming $\chi_{\text{solvent-p}}(T) = \chi_{\text{solvent-p}}(293)(293/T)$. Bottom: zoom-in view of the red curves.

Section IV. Determination of $R_{h,eq}$ of the PEC Aggregates by DLS

DLS Autocorrelation Functions and Fit

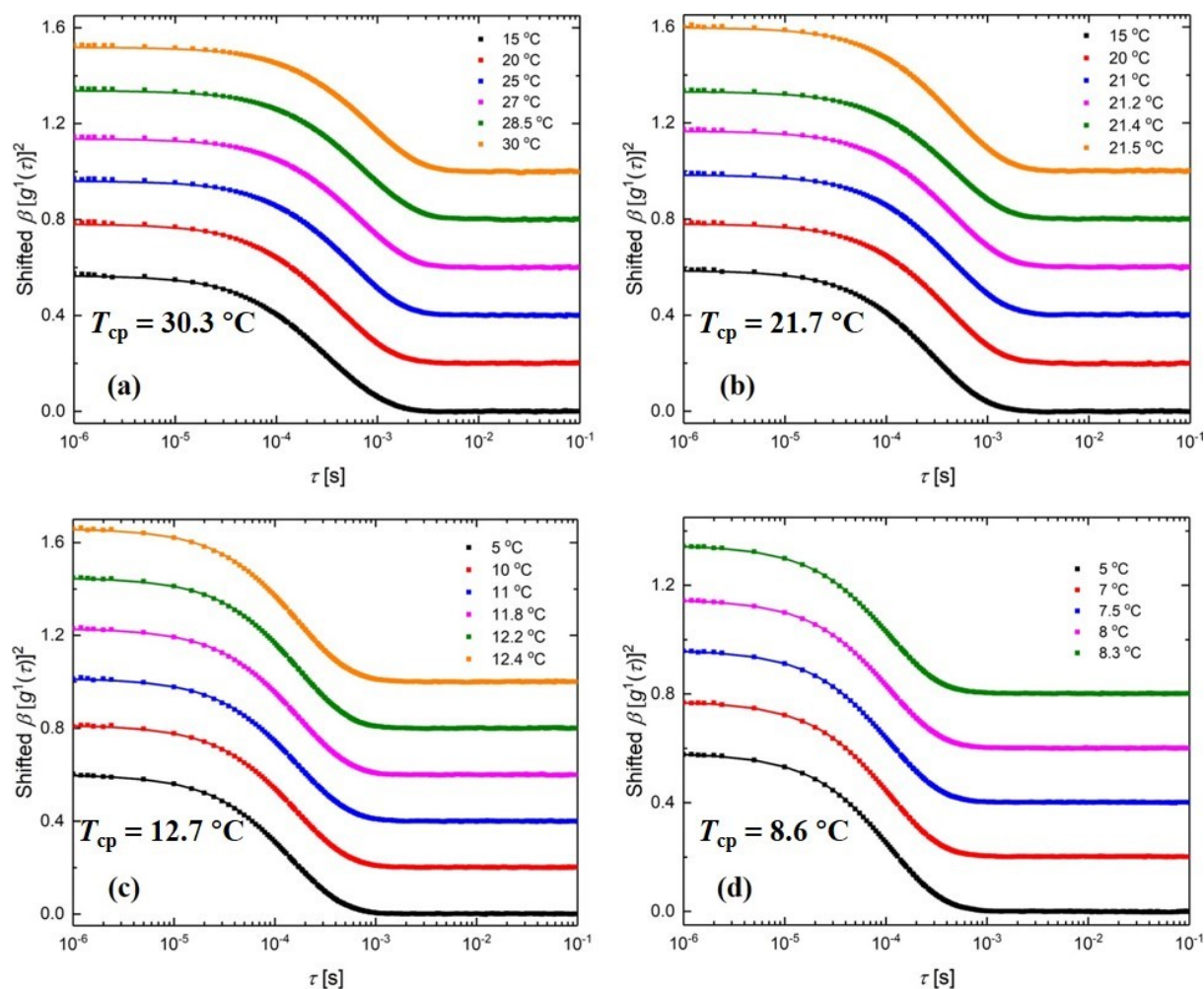


Figure S10. The baseline-subtracted autocorrelation functions of KPSS-PDADMAB complexes in water with $c_s = 1.80$ mol/L and $c_p =$ (a) 0.3 mol/L, (b) 0.2 mol/L, (c) 0.1 mol/L, and (d) 0.05 mol/L. The solid lines are best fit to the quadratic cumulant function, $\beta[g_1(\tau)]^2 = A \cdot \exp[-2\Gamma\tau(1 + \mu_2\tau^2/2)]$. Within each group, every curve is shifted by 0.2, for clarity. The cloud point temperatures (T_{cp}) of each sample were noted, marking the upper bound of each measurement.

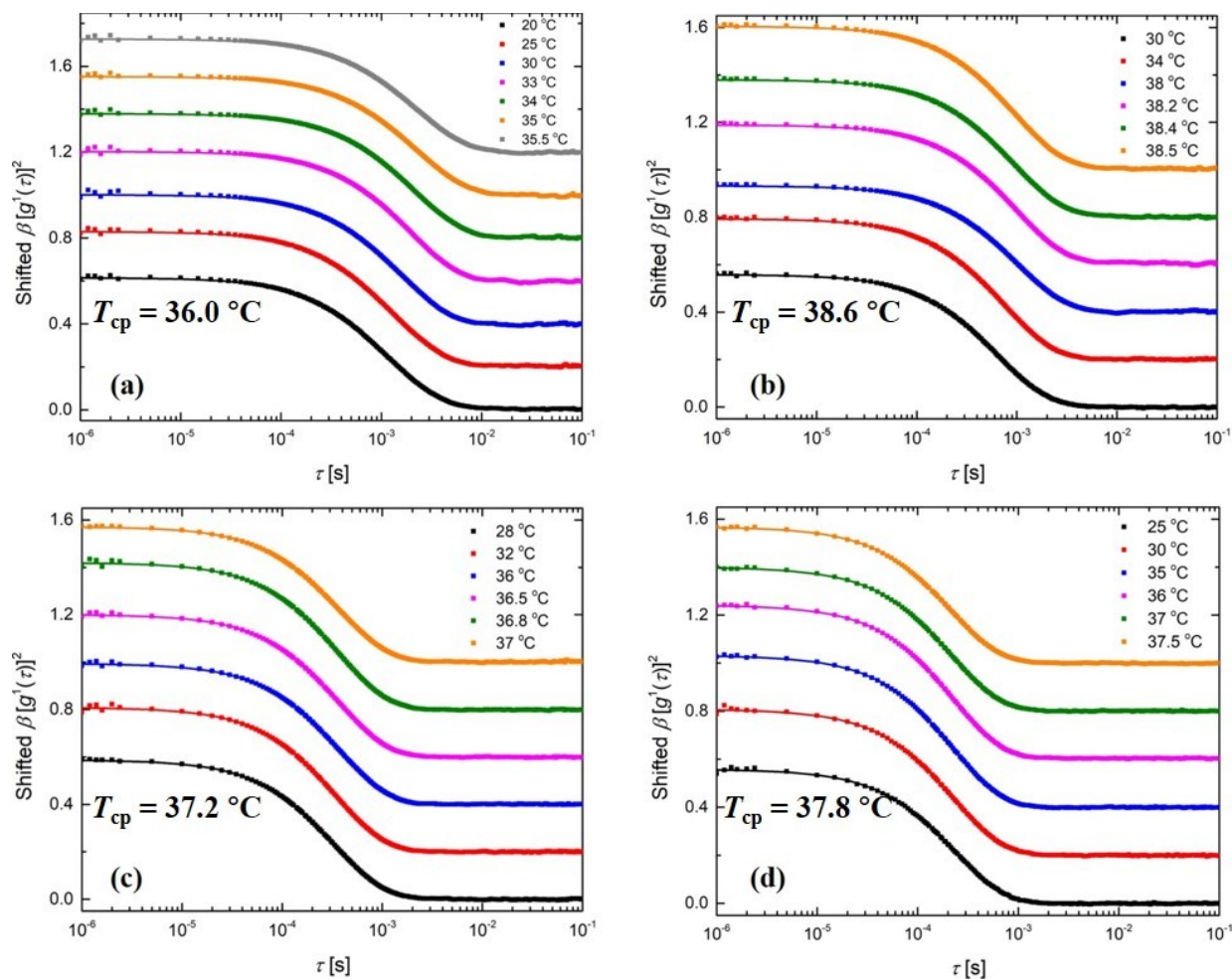


Figure S11. The baseline-subtracted autocorrelation functions of KPSS-PDADMAB complexes in EG/H₂O=50/50 with $c_s = 1.10$ mol/L and $c_p =$ (a) 0.3 mol/L, (b) 0.2 mol/L, (c) 0.1 mol/L, and (d) 0.05 mol/L. The same data processing protocol as Figure S10 was used.

Viscosity of the Mixed Solvents

The temperature-dependent viscosity of EG/H₂O mixtures, $\eta(T)$, was estimated by interpolation of literature data with respect to molar fractions (x_{EG}).¹⁴ Due to asymmetry in molecular weights of the two solvents, the cosolvent with $\varphi_{EG}^S = 0.50$ is equal to $x_{EG} = 0.244$, and its $\eta(T)$ values (on the log scale) at four specific temperatures were determined by interpolation of the literature data, as shown in Figure S12. The viscosities of $\varphi_{EG}^S = 0.50$ at other intermediate temperatures were again estimated by interpolation using a third-order polynomial relation.

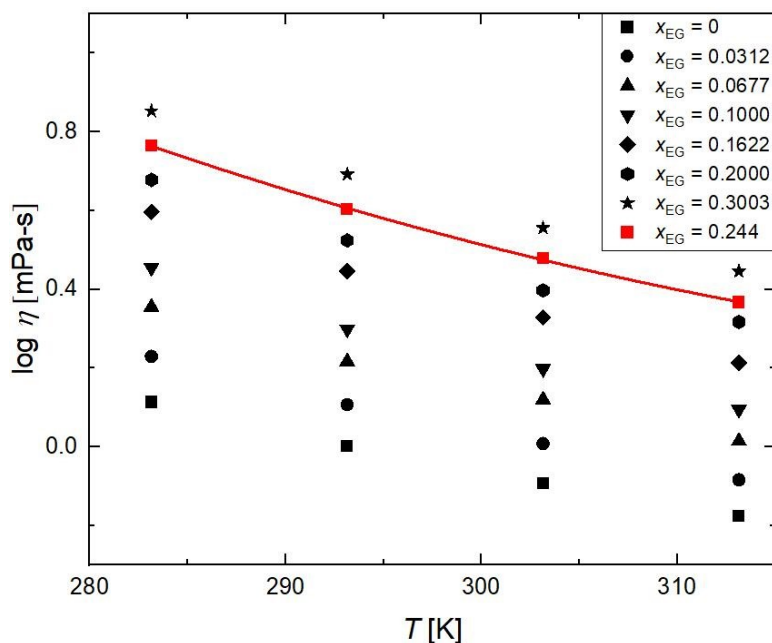


Figure S12. Temperature-dependent viscosities $[\eta(T)]$ of EG/H₂O mixtures as reported by Tsierekzos *et al.*¹⁴ The black symbols are from the reference, which cover $x_{EG} = 0$ to 0.3, corresponding to ϕ_{EG}^S of 0 to 0.59. The red symbols are interpolation of black symbols to $x_{EG} = 0.244$ (corresponding to ϕ_{EG}^S of 0.50), and the red line is the best cubic fit to the data points.

References

- (1) Kirkup, L.; Frenkel, B. *An Introduction to Uncertainty in Measurement*, Cambridge University Press, Cambridge, UK (2006).
- (2) van Krevelen, D. W.; te Nijenhuis, K. *Properties of Polymers (4th Ed)*, Elsevier (2009).
- (3) Ferrell, W. H.; Kushner, D. I.; Hickner, M. A. Investigation of polymer–solvent interactions in poly(styrene sulfonate) thin films. *J. Polym. Sci. Part B* **2017**, *55*, 1365–1372.
- (4) Lindvig, T.; Michelsen, M. L.; Kontogeorgis, G. M. A Flory–Huggins model based on the Hansen solubility parameters. *Fluid Phase Equilibria* **2002**, *203*, 247–260.
- (5) Venkataraman, S.; Wei, G.; Mineart, K. P.; Hedrick, J. L.; Prabhu, V. M.; Yang, Y. Y. The effect of solvent quality on pathway-dependent solution-state self-assembly of an amphiphilic diblock copolymer. *J. Appl. Phys.* **2020**, *127*(12), 125104.
- (6) Overbeek, J. T. G.; Voorn, M. J. Phase separation in polyelectrolyte solutions. Theory of complex coacervation. *J. Cell. Physiol.* **1957**, *49*, 7-26.
- (7) Audus, D. J.; Ali, S.; Rumyantsev, A. M.; Ma, Y.; de Pablo, J. J.; Prabhu, V. M. Molecular

Mass Dependence of Interfacial Tension in Complex Coacervation. *Phys. Rev. Lett.* **2021**, *126*, 237801.

(8) Bass, S. J.; Nathan, W. I.; Meighan, R. M.; Cole, R. H. Dielectric Properties of Alkyl Amides. II. Liquid Dielectric Constant and Loss. *J. Phys. Chem.* **1964**, *68*, 3, 509–515.

(9) Leader, G. R.; Gormley, J. F. The Dielectric Constant of N-Methylamides. *J. Am. Chem. Soc.* **1951**, *73*, 12, 5731–5733.

(10) Malmberg, C. G.; Maryott, A. A. Dielectric constant of water from 0° to 100 °C. *J. Res. Natl. Bur. Stand.* **1956**, *56*, 1-8.

(11) Akerlof, G. Dielectric constants of some organic solvent-water mixtures at various temperatures. *J. Am. Chem. Soc.* **1932**, *54*, 11, 4125–4139.

(12) Rohdewald, P.; Moldner, M. Dielectric Constants of Amide-Water Systems. *J. Phys. Chem.* **1973**, *77*, 3, 373-377.

(13) Sengwa, R. J.; Sankhla, S.; Khatri, V. Static dielectric constants of the binary mixtures of N-methylformamide with water, ethyl alcohol, ethylene glycol, dimethylsulphoxide, acetone and 1,4-dioxane. *Philos. Mag. Lett.* **2010**, *90*, 7, 463–470.

(14) Tsierkezos, N. G.; Molinou, I. E. Thermodynamic Properties of Water + Ethylene Glycol at 283.15, 293.15, 303.15, and 313.15 K. *J. Chem. Eng. Data* **1998**, *43*, 989-993.